Effect of Aging on Internal Stress and Fatigue Fracture of Poly(4-methyl Pentene-1)

G. J. SANDILANDS* and J. R. WHITE, *Department of Metallurgy and Engineering Materials, University of Newcastle upon Tyne, Newcastle upon Tyne NE1 7RU, United Kingdom*

Synopsis

The fatigue fracture behaviour of injection-molded poly(4 methyl pentene-1) has been investigated. Crack growth rate experiments have been conducted on notched specimens after room temperature aging, after annealing at 175°C, and after prolonged cyclic loading prior to notching. Residual stress profiles have been determined for specimens in each of these states, and the crack growth data have been discussed with reference to differences in residual stresses. Annealing caused the reversal of the sense of the residual stresses, and a significant change in stress distribution was found for specimens freshly removed from prolonged storage at −18°C. Scanning electron microscopy of fracture surfaces revealed fibrillar features essentially similar to those found with other semicrystalline polymers.

INTRODUCTION

Polymeric components change their properties with time especially when fabricated by a process such as injection molding in which the material cools rapidly during solidification. Important mechanical properties such as the creep and fracture behavior show marked aging dependence. Large temperature gradients normally exist within an article during injection molding so that the material at each location has a different thermal history. Another consequence is that residual stresses develop during solidification.[1] The as-molded material is in a nonequilibrium state and moves slowly towards a more stable condition causing the properties to change even when stored at room temperature. This is true even with glassy polymers held below their glass transition temperature T_g.[2] Crystallizing polymers also display an aging effect.[3-8] For many crystallizing polymers, T_g is below room temperature and molecular motion is fairly easy in noncrystallized regions, allowing relaxation of residual stresses and some further crystallization. The ultimate extent of aging, as determined by changes in structure or property, depends on temperature, as does the rate at which aging occurs. Finally, aging is influenced by stress through stress-aided thermal activation of molecular conformation changes and as a result of the creation of "free volume" which permits easier relaxation.[2] The effects of static and dynamic loads on aging have been discussed by Struik.[2]

The state of the material, as modified by aging, can be expected to influence the fracture behavior. A separate effect will be that connected with the residual stresses which are themselves modified by aging. The residual

* Present address: Department of Materials Technology, Brunel University, Uxbridge, Middlesex UB8 3PH, United Kingdom.

Journal of Applied Polymer Science, Vol. 30, 4771–4792 (1985)
 CCC 0021-8995/85/124771-22$04.00

stresses add algebraically to the applied stress so that in regions containing compressive residual stresses a higher applied (tensile) stress will be required for crack initiation or propagation. Conversely, regions containing tensile residual stresses can be expected to fail at lower applied stresses than would be required in the absence of residual stresses.

Thus, when attempting to assess the fracture behavior of an injection molding, it is necessary to take into account the specimen history, which must include processing conditions and all post-processing conditioning, both thermal and mechanical. The specimen history will lead to a set of characteristics, and to adequately specify the material it appears that the following should all be known: the structure and morphology; molecular orientation; residual stresses; density; thermal state (enthalpy). These characteristics might be expected to determine in turn the fracture behavior of the material through their influence on crack initiation, including the site of initiation as well as the stress and time under stress (or, in the case of fatigue, stress range and number of cycles) to initiate fracture, on crack propagation, and on the mechanism of fracture. It must also be recognized that in an injection molding not only the morphology and the residual stress vary according to position but also molecular orientation, density, and enthalpy. Clearly, the analysis of the fracture behavior of injection moldings is extremely complex, and for this reason many fundamental studies on the fracture properties of polymers have been conducted on samples prepared by some other technique designed to reduce the number of variables and to produce a more nearly homogeneous test piece. For example, studies on fatigue fracture of polyethylene have been conducted on samples recrystallized in a tight-fitting mold and slow cooled, and then left to age for several weeks.[9-11]

The widespread use of injection-molded components, often in critical load-bearing applications, has made it necessary to study the fracture characteristics of polymers in injection-molded form. In the work reported here the test programme was organized to obtain information primarily on the influence of residual stresses and aging on the fatigue fracture behavior of poly(4-methyl pentene-1) in injection-molded form. The objectives of an investigation by Mandell et al. were fairly similar, though in this case the material studied was polysulfone.[12] One type of experiment introduced in the research reported here was to examine the effect of cyclic deformation on subsequent crack propagation behavior. This was done by cyclically loading an unnotched test piece, and then introducing a notch and subjecting the specimen to further cyclic loading. It is inevitable that under normal circumstances a fatigue crack grows into material that has suffered progressively more load cycles before the crack front reaches it. The purpose of experiments of the kind just outlined was to test whether this is important for they permit comparison of the fatigue crack growth rate at a specific location (removing geometric effects) using a specific load cycle (stress range, maximum stress, frequency) but in material which has suffered different amounts of load cycling. The effect of load cycling on subsequent fracture behavior was examined by Sadd et al.[13] for poly(methyl methacrylate), but they conducted the second stage (failure) test by monotonic loading rather than by notching and further cyclic loading as in the present work.

Poly(4-methyl pentene-1) (P4MP1) was chosen for the present work, partly because it is unique in that it is both highly transparent and semicrystalline. Even at 50% crystallinity (a typical level) P4MP1 has a transparency comparable to that of an amorphous glassy polymer, and this permits visual observation of the crack front. Another reason for this choice of material was that a detailed study of the morphology of P4MP1 in injection-molded form has already been published.[14,15]

EXPERIMENTAL

Specimen Preparation

Specimens were made from P4MP1 produced by the Mitsui Petrochemical Industries under the trade name of TPX (formerly an ICI trade name) grade RT-18. (This material is a commercial product and may contain some copolymer to enhance its physical or mechanical properties). Straight bars measuring approximately 190 × 12.5 × 3 mm were injection-molded on a Butler-Smith 100/60 reciprocating screw machine using a single end-gated cavity. The following conditions were found to produce moldings free from visual defects (sink marks, etc.) and were used throughout: tool temperature 67°C; nozzle temperature 295°C; barrel forward zone temperature 280°C; barrel rear zone temperature 270°C; injection pressure (indicated machine pressure) 118 MPa; injection time 5 s; cooling time 30 s. Specimens were molded in two separate batches, and collection of those used for the tests reported here did not commence until the machine had undergone at least 10 cycles without any adjustment of settings or any change in the indicated conditions. Specimens were numbered sequentially so that any drift in property could be detected retrospectively.

Specimen Conditioning

Specimens were stored either in a laboratory in which there was no humidity control, or in a freezer unit controlled at about −18°C. The purpose of subambient storage was to minimize the effect of aging. P4MP1 has a reported T_g of + 18°C and storage at −18°C should therefore retard all conformational changes. One group of specimens was annealed at 175°C for 24 h and allowed to cool slowly in the oven. Mechanical preconditioning was conducted on unnotched samples using tensile load cycling (zero to 6.45 MN/m^2) at 0.083 Hz at 25°C. This was continued for 150,000 cycles and did not promote the formation of any visible defects.

Residual Stress Measurement

The residual stress distributions in bars conditioned by each of the methods outlined in the previous section were determined using the layer removal procedure.[1,16,17] In this procedure thin uniform layers are removed from the bar, resulting in an imbalance in the stresses, causing the bar to bend. The bar curvature is measured at each removal step using a non contact method based on the optical lever principle,[8,16] and then plotted versus the depth removed. From this plot the routine derived by Treuting

and Read[17] is used to generate a plot of residual stress vs. position in the bar. For biaxial stresses, giving rise to curvatures ρ_x and ρ_y in orthogonal directions, the stress parallel to the x-axis is given by

$$\sigma_{i,x}(z_1) = \frac{-E}{6(1-\nu^2)}\left\{(z_0 + z_1)^2\left[\frac{d\rho_x(z_1)}{dz_1} + \frac{\nu d\rho_y(z_1)}{dz_1}\right] + 4(z_0 + z_1)\right. \quad (1)$$

$$\left.\left[\rho_x(z_1) + \nu\rho_y(z_1)\right] - 2\int_{z_1}^{z_0}\left[\rho_x(z) + \nu\rho_y(z)\right] dz\right\}$$

where E and ν are the Young's modulus and Poisson's ratio for the bar, both assumed to be uniform, $2z_0$ is the bar thickness, and z_1 is the location of the machined surface measured from the plane which was located at the bar center prior to machining. The expression for $\sigma_{i,y}$ is obtained by interchanging subscripts x and y. This formula (1) simplifies for several common cases.[1] For example, in the case of equibiaxial stresses $\sigma_{i,x} = \sigma_{i,y}$ and $\rho_x = \rho_y = \rho$ (say) and

$$\sigma_{i,x} = \frac{-E}{6(1-\nu)}\left[(z_0 + z_1)^2\frac{d\rho(z_1)}{dz_1} + 4(z_0 + z_1)\rho(z_1) - 2\int_{z_1}^{z_0}\rho(z)\,dz\right] \quad (2)$$

In the present work the use of bars only 12.5 mm wide made measurement of the curvature perpendicular to the bar axis (ρ_y) difficult to achieve; visual inspection indicated that the curvature in this direction was small, and by setting $\rho_y = 0$ in eq. (1) the Treuting and Read formula becomes

$$\sigma_{i,x} = \frac{-E}{6(1-\nu^2)}\left[(z_0 + z_1)^2\frac{d\rho(z_1)}{dz_1} + 4(z_0 + z_1)\rho(z_1) - \int_{z_1}^{z_0}\rho(z)\,dz\right] \quad (3)$$

This is the form used to generate the stress profiles presented here, using $E = 2$ GN/m^2 and $\nu = 0.4$. [Note that this implies anisotropy of residual stresses, with higher values in the bar axis ($x-$) direction than transverse to it but it does not imply that σ_y is zero[1].]

Fatigue Testing

Details of the design of the fatigue rigs used in this investigation are found elsewhere.[18] The special features of the machines are: (i) an electromechanical system enabling the use of load control conditions in the presence of dynamic creep and (ii) automatic photographic recording of the crack. The creep compensation apparatus is a further development of the system described by Teh et al.[9] and permits the construction of a dedicated fatigue rig capable of controlled testing of a kind which normally requires much more expensive equipment. If the specimen changes length during a test, this is sensed and the control system sends a command to a servo motor

which moves the crosshead to which the nondriven end of the specimen is attached until the preset maximum load is recovered. The displacement of the nondriven end of the specimen is thus taken to be the accumulated dynamic creep and is monitored using a dial gauge which is read periodically during the test.

Automatic photographic recording of the crack is achieved using a Nikon FE Series 35 mm camera with motor-driven film advance, triggered externally. The trigger signal requires the opening of two gates, the first provided by a purpose-built timer circuit set typically at a 30 min interval, and the second provided by a microswitch operating directly off the machine main drive unit. The microswitch is set to activate the exposure at the phase of the cycle at which the crack is most visible and with P4MP1 was at the maximum tension limit. (Crack visibility is also critically dependent on the siting of the flash unit, which must be established by experiment). These systems were designed and built before the availability of microprocessor technology which will permit further improvements in the basic design of the equipment.

The camera is fitted with a 90 mm macrolens and extension rings giving a slightly enlarged image on the film. The cycle counter is mounted alongside the specimen so that the test cycle number is recorded each exposure insuring against faulty time intervals and simplifying logging and storage of the information. The crack length is measured directly from the film using a travelling microscope.

"Perspex" specimen enclosures were built for each of the rigs and kept at a uniform controlled temperature by means of air propelled by an in-line fan over a resistance heater located in a duct in parallel with the enclosure. Much of the air recirculates, helping to maintain a constant temperature. The heater is controlled by a West Gardian Q3X controller and the temperature sensor, a resistance thermometer in a sheath perforated to permit air circulation, is located close to the specimen. Part of the tie bars of the machine test frame are contained within the constant temperature enclosure, and this reduces the effect of changes in room temperature through thermal expansion and contraction of the test frame. The design is similar to that developed by Haworth for stress relaxation rigs.[19]

The stress is monitored using a Pye-Ether UF2 load cell and strain is monitored using a displacement transducer connected directly across the specimen grips. The tests reported here were conducted at 25°C in uniaxial tension with minimum stress set to zero using a frequency of 0.083 Hz. The bars were tested in the form in which they were molded, but were provided with an edge notch at the center. This was made using a razor blade mounted on a special jig to ensure reproducible notches with controlled penetration. A fresh region of razor blade was used for each specimen, but the jig was designed to allow five specimens to be notched by each blade, using a different section each time.[18] Although the specimen geometry is not ideal for fracture mechanics analysis, it was chosen because it is convenient for residual stress assessment (by the layer removal procedure) and because such straight bars are relatively simple to characterize while at the same time retain the important features of injection moldings which we wish to investigate.

Scanning Electron Microscopy

Selected fracture surfaces were mounted on scanning electron microscope stubs and gold-coated for inspection in the scanning electron microscope. An accelerating voltage of 7.5 kV was used together with fairly low beam currents, appropriate to secondary electron imaging, and under these conditions observation was possible without any apparent production of visible beam damage.

RESULTS

Residual Stress Distributions

For all conditions tested the bars were found to be straight prior to layer removals, and it is reasonable to assume that they contained a symmetric stress distribution. Results are therefore shown for half of the bar thickness. In each case the curvature plot $\rho(z_1)$ is shown as well as the stress distribution derived by the Treuting and Read analysis, $\sigma_i(z_1)$. We have chosen this method of presentation as standard because (i) there is an element of subjectivity in constructing the $\rho(z_1)$ line from the data points and any error will influence the results of the Treuting and Read analysis and (ii) if there is a nonuniform modulus this will influence the shape of the $\rho(z_1)$ curve.[20] Hence for some purposes the $\rho(z_1)$ plot contains more information than the $\sigma_i(z_1)$ curve, though we shall discuss the results in terms of the stress distributions derived.

Residual stress profiles are shown for P4MP1 in the following states: as-molded (Fig. 1); aged for $\sim$ 1 month at room temperature (Fig. 2); annealed for 24 h at 175°C (Fig. 3); stored for 14 months at −18°C (Fig. 4); and mechanically conditioned by cycling at 0–6.45 MN/m^2 at 0.083 Hz for 150,000 cycles at 25°C (Fig. 5). The residual stress profile in an as-molded bar is predicted by simple solidification theory to be parabolic, with tensile stresses in the interior balanced by compressive stresses near to the surface.[21] Theories which take into account the viscoelastic nature of polymers show general agreement, but with detailed modification to the parabolic profile.[22–25] The stress profile obtained for "as-molded" P4MP1 was obtained within 24 h of molding and shows considerable departure from parabolic (Fig. 1). The stress is compressive near to the surface, rising steeply in magnitude as is usual. Stress reversal occurs at about 0.25 mm from the surface; the stress continues to rise to a tensile maximum at about 0.6 mm from the surface, and then falls to a very low value ($\sim$ zero) about 1.1 mm from the surface, rising again to a maximum at the bar center. Maxima located near to the point of stress reversal have been observed before for other materials,[16] but we have not found such a pronounced sequence of maximum–minimum–maximum in a half bar of any other material. The stress distribution obtained for specimens aged at room temperature for a month (Fig. 2) is similar in shape to that obtained for as-molded samples, but is flattened somewhat, with a less steep rise in the magnitude of the compressive stress near to the surface and a smoother profile in the (tensile) interior.

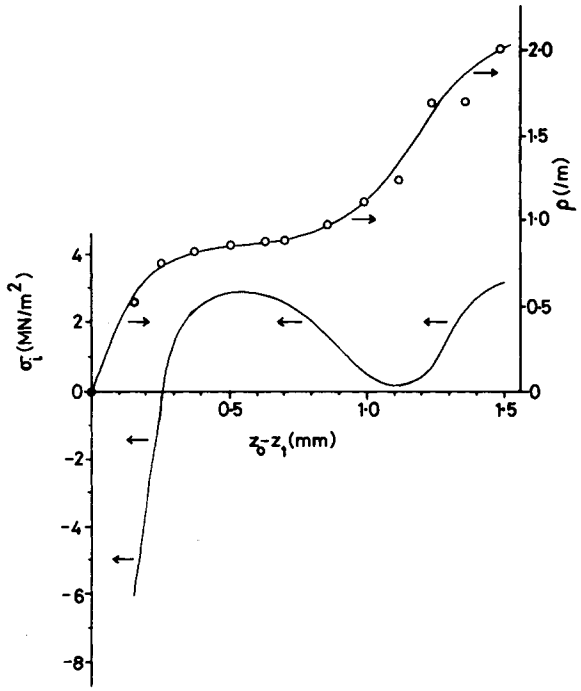

Fig. 1. Layer removal analysis obtained within 24 h of molding a 3 mm thick bar from P4MP1. The curvature ρ obtained for various depth removals ($z_0 - z_1$) is shown in the upper curve, and the computed residual stress profile (σ_i) is shown as the lower curve.

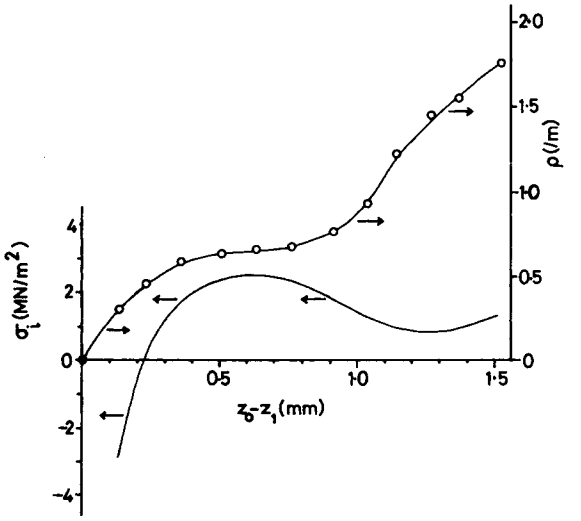

Fig. 2. Layer removal analysis for P4MP1 aged at room temperature.

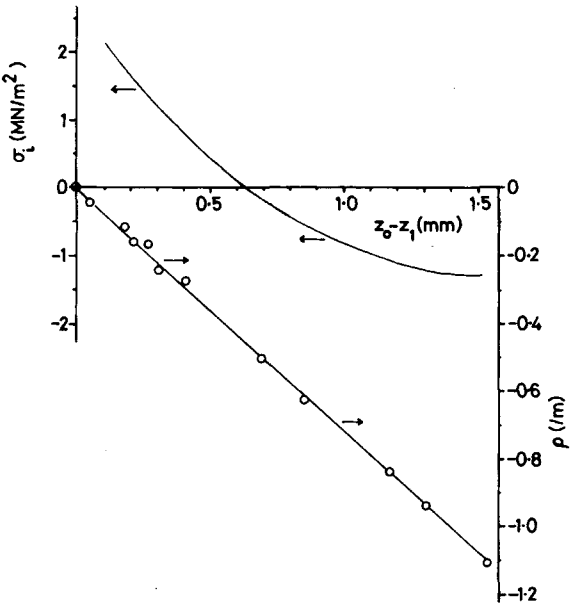

Fig. 3. Layer removal analysis for P4MP1 annealed at 175°C.

The result obtained from annealed specimens shows an unexpected stress profile with tensile stresses near to the surface, balanced by compressive stresses in the interior (Fig. 3). The curvature plot is linear and passes through the origin and as such corresponds exactly to a parabolic stress distribution,[16] though with the stress sense inverted when compared to that normally observed.

Even more surprising is the result obtained with specimens stored at −18°C (Fig. 4). The sense of bending initially indicated compressive stresses

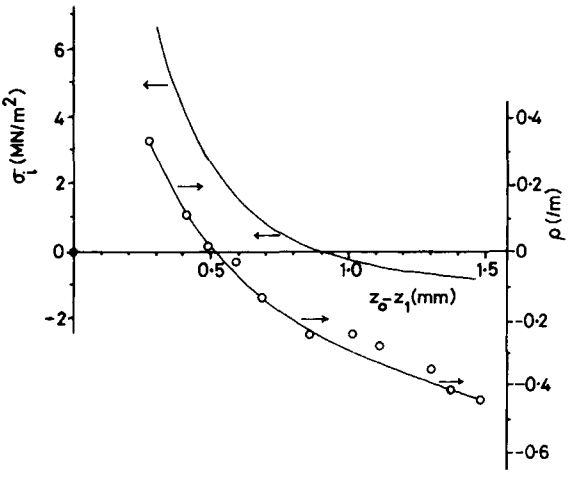

Fig. 4. Layer removal analysis for P4MP1 after prolonged storage at −18°C and before allowing room temperature recovery.

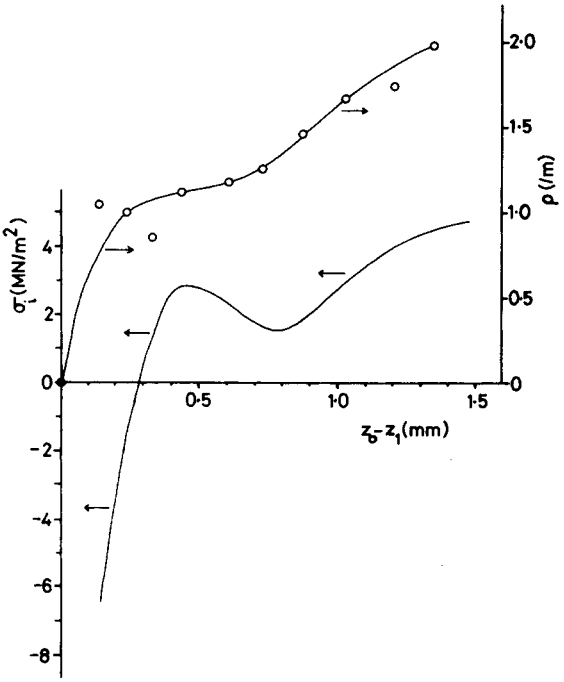

Fig. 5. Layer removal analysis for P4MP1 after 150,000 load applications (peak stress 6.45 MN/m²).

near the surface [not shown in Fig. 4 because of the difficulty of accurately locating the initial part of the curvature plot from which σ_i at small $(z_0 - z_1)$ must be derived]. The curvature then began to reduce and eventually reversed sign (after the removal of $\sim$ 0.6 mm). Analysis shows that this corresponds to tensile stresses in the region on either side of $(z_0 - z_1) = 0.6$ mm, and that weak compressive stresses are present near to the bar center. The stress profile shown in Figure 4 is of unknown accuracy and should be treated with caution for the following reasons. Firstly, as mentioned above, compressive stresses are present near to the surface; but these could not be estimated with confidence and are therefore not shown in Figure 4. The absence of this part of the stress distribution is the principal reason why the tensile and compressive regions do not balance. Any error in the location of the $\rho(z_1)$ curve will be carried forward into the analyzed σ_i profile for parts of the bar remote from the surface through the integral term in eqs. (1)–(3), so even for $(z_0 - z_1) > 0.25$ mm the σ_i profile may not be accurate. Furthermore, the bars age quite rapidly on removing them from cold storage (see below), and the stress distribution may change by a considerable and unknown amount during the execution of the layer removal procedure, hence introducing further uncertainty. Figure 4 has been included here to illustrate our discovery of an unexpected phenomenon, but it must be admitted that the absolute stress levels are most uncertain. In a separate experiment a bar was removed from the −18°C freezer and then aged at 25°C for 50 h in a vacuum oven before milling away layers. This bar showed a return to a more conventional stress

distribution, with only one reversal of the sense of curvature. Hence a significant part of the change in stress distribution that occurs during storage at depressed temperature (compare Figures 1 and 4) is reversible, and the anomalous aspects are removed on ageing at room temperature.

Finally, Figure 5 shows the results obtained with specimens which had been mechanically conditioned by cyclic loading. The analyzed stress profile displays stress magnitudes higher than those found in the as-molded state (Fig. 1). The effect of mechanical conditioning has therefore been the opposite of that promoted by aging in the absence of any applied stress (compare with Fig. 2).

Fatigue Testing

Crack growth data are presented in the manner described by Teh et al.,[10] which was developed from an earlier study by Andrews and Walker.[4] The procedure is based on the empirical relationship that relates crack growth rate to a fracture mechanics parameter T:

$$\frac{dc}{dN} = BT^n \tag{4}$$

where c is the crack length, N is the number of cycles, and B and n are specific to the material used but are dependent also on the test conditions particularly the temperature. For an edge crack the fracture mechanics parameter can be written

$$T = kcW_0 \tag{5}$$

where W_0 is the input energy density at points remote from the crack and k is a function that varies slowly with strain. W_0 is thus the work done on unit volume of material during monotonic loading in the absence of a crack. Two methods for measuring W_0 as a function of the cyclic strain maximum are described by Teh et al.[10] and both have been used here to obtain a calibration curve for W_0 in terms of the strain. Extremely good agreement was found between the results of the two methods, (Figs. 6 and 7), which use data obtained during the fatigue tests ("notched specimens") and independent tests on unnotched specimens, respectively. The value of k can also be obtained from the cyclic loading hysteresis loops obtained during the fatigue tests[10,18] using a plot of input energy vs. c^2. A second method of measuring k uses monotonic load extension curves obtained for a series of specimens with edge cracks of different lengths.[10,18] Both methods were used and gave good agreement (Fig. 8). k is seen to vary slowly, in agreement with the initial hypothesis. The value of k is much greater than that obtained for elastomers ($1 \leq k \leq \pi$),[26,27] but is fairly similar in magnitude and behavior to the results obtained with low density polyethylene.[10]

Combination of eqs. (4) and (5) predicts that a plot of $\log(dc/dN)$ vs. $\log(kcW_0)$ should produce a straight line, and results are shown for tests conducted on bars aged at room temperature (Fig. 9), after annealing (Fig. 10), and after (cyclic) mechanical preconditioning (Fig. 11). It was intended to conduct tests on specimens in the "as-molded" state, using specimens

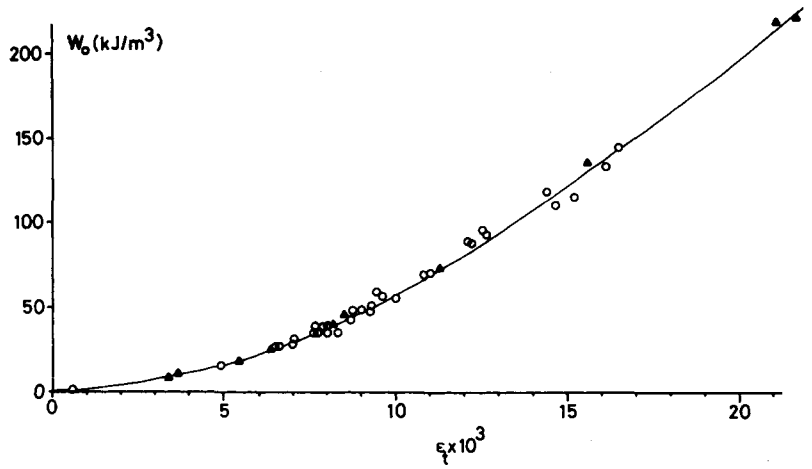

Fig. 6. Relationship between input strain energy density W_0, and maximum tensile strain ϵ_t, for aged P4MP1 obtained from tests using unnotched specimens (▲) and notched specimens (0).

preserved in this state by storing at low temperature. That this could not be achieved is clear from the residual stress results presented above which showed that unexpected changes developed at −18°C. A further difficulty was that serious grip slipping occurred with all specimens taken from cold storage and tested as soon as they had reached room temperature equilibrium. A large amount of scatter is evident in Figures 9–11, but this is normally found with fatigue tests on polymers. Other workers often plot crack growth rate as a function of the maximum stress intensity factor or the stress intensity factor range during load cycling,[28] but this method does not alter the extent of the scatter. On comparing the results shown in

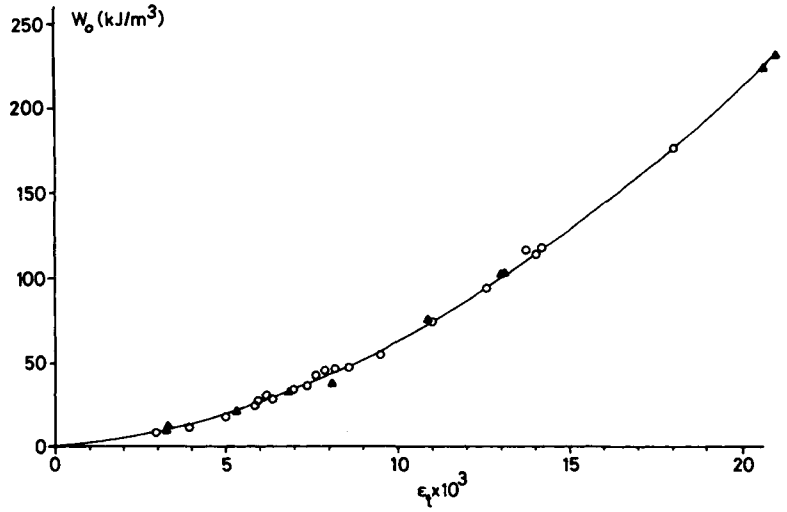

Fig. 7. Relationship between W_0 and ϵ_t for annealed P4MP1 obtained using unnotched specimens (▲) and notched specimens (0).

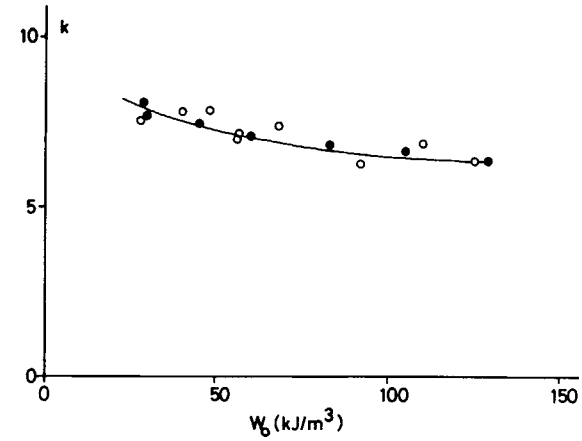

Fig. 8. Parameter k as a function of W_0 obtained using fatigue test hysteresis loops (0) and using monotonic load extension curves (●).

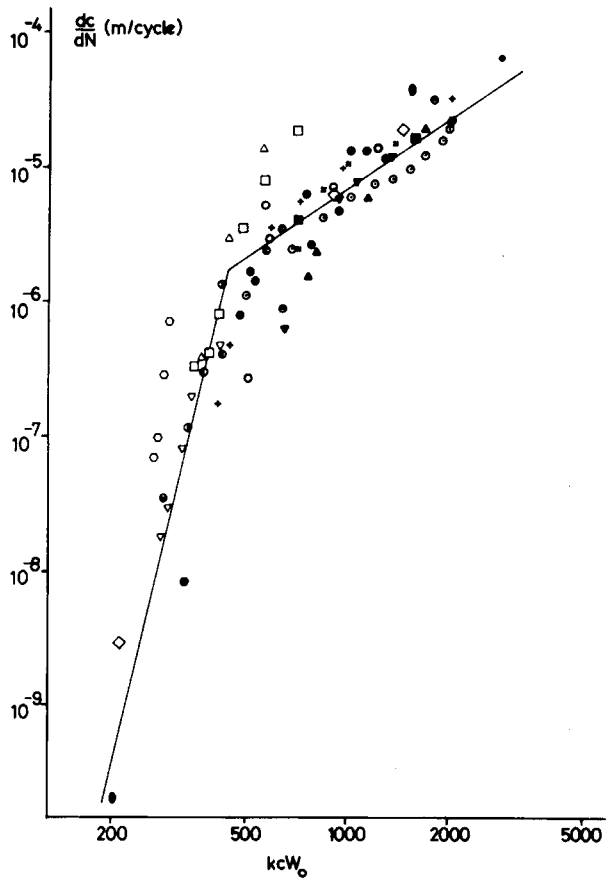

Fig. 9. Crack growth rate data for specimens aged at room temperature. Each test provides several data points, and each data point provided by the same test is represented by the same symbol.

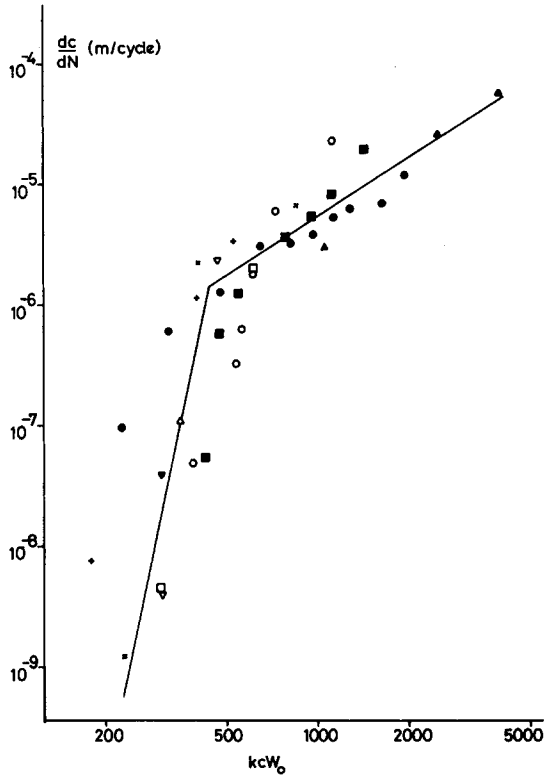

Fig. 10. Crack growth rate data for annealed specimens.

Figures 9–11 with those published elsewhere, it should be noted that we have chosen to expand the horizontal axis [$\log(kcW_0)$] compared to that used by many others, and this tends to emphasize the scatter.

The crack propagation for P4MP1 in all of the three states tested shows a two-stage characteristic. Two- or three-stage crack growth rate characteristics have been found before, with low density polyethylene,[4,10] vinyl urethane polymers,[29] and others. (It has been suggested that stress corrosion cracking in an aggressive environment such as a detergent may promote two- or three-stage cracking,[30–32] although it has not been shown that the presence of such a cracking or crazing agent is an exclusive requisite.)

The values of the index n [eq.(4)] for the two stages are as follows. Aged samples: first stage $n_I = 10.3$, second stage $n_{II} = 1.7$. Annealed samples: $n_I = 10.1$, $n_{II} = 1.6$. Mechanically preconditioned samples: $n_I = 10.1$, $n_{II} = 1.7$. The characteristics for all three states are shown together in Figure 12. The changeover from stage I to stage II occurs at approximately the same value of kcW_0 in each case, approximately 437 ($\log kcW_0 \sim 2.64$).

Fractography

Fatigue striations were clearly visible near to the end of the fatigue life when the crack advanced in large increments each cycle. Prenotched samples cycled at high strain amplitudes giving low fatigue lives developed this

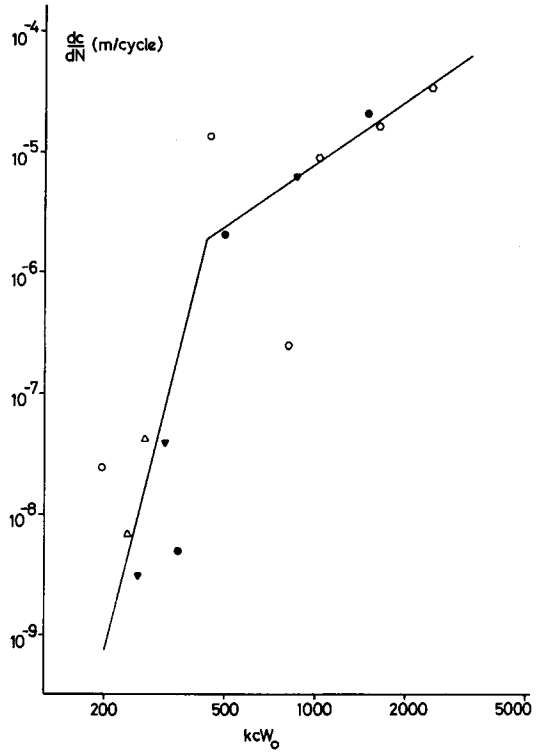

Fig. 11. Crack growth rate data for specimens which had been mechanically preconditioned (by cyclic loading) prior to notching.

kind of fatigue striation pattern near the beginning (Fig. 13). At high magnification it appears that the striations correspond to voids which line up parallel to the fracture front (Fig. 14). With the exception of specimens cycled at high strain amplitudes, causing immediate development of the striation pattern, it was found that near the notch the fracture surface has a voided fibrous appearance (Fig. 15). At a more advanced stage of crack growth the fracture surface appearance is much less fibrous (Fig. 16). A limited number of fracture surfaces were obtained in uniaxial tension, using both notched and unnotched samples, for comparison with the fatigue fracture surfaces. The unnotched sample showed the development of voiding (Fig. 17). When notched samples broken in uniaxial tension were viewed at high magnification, the fracture surface morphology in regions remote from the notch was reminiscent of that obtained at a similar location in fatigue fracture surfaces (Fig. 18; cf. Fig. 16) and showed very little evidence for voiding. At low magnification uniaxial tension fracture surfaces were free from striations and thus easily distinguished from fatigue fracture surfaces. Near to the notch significant voiding can be found in the uniaxial tension fracture surface (Fig. 19) but is not developed to the extent seen in the corresponding position on fatigue fracture surfaces (e.g., Fig. 15).

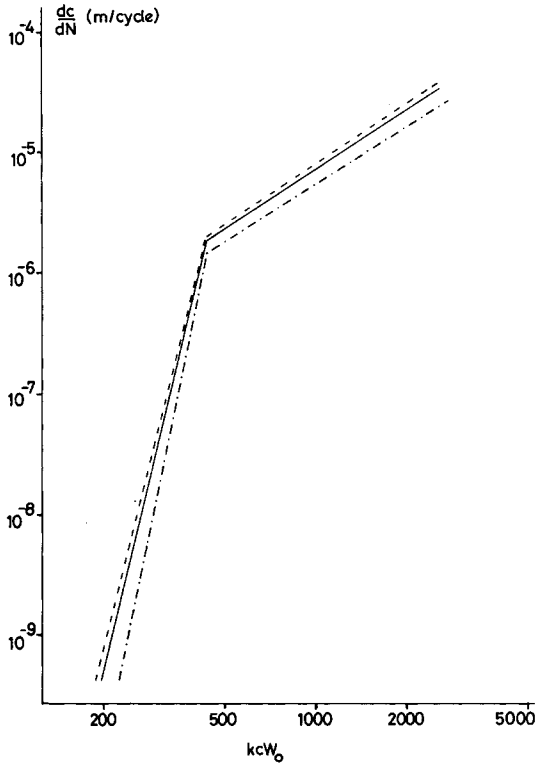

Fig. 12. Crack growth rate data reproduced from Figures 9–11: (——) aged; (· - ·) annealed; (- - -) mechanically preconditioned.

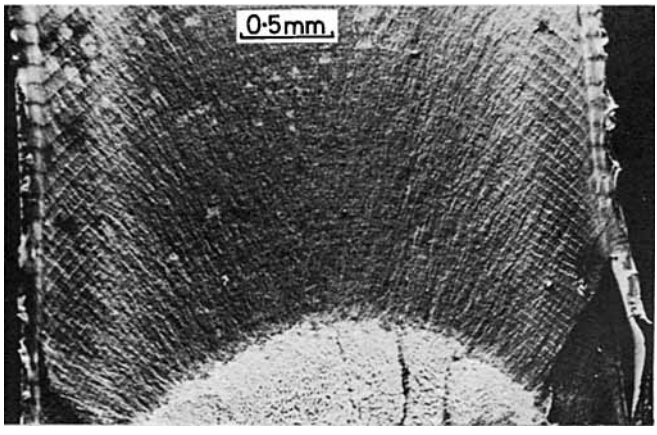

Fig. 13. Secodary electron image (SEI) of an aged sample fatigue tested at high strain, causing failure in 55 cycles, showing prominent fatigue striations.

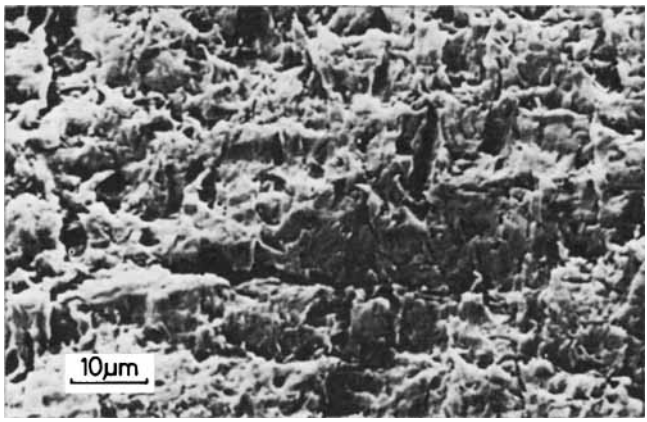

Fig. 14. High magnification SEI of a region containing fatigue striations running horizontally.

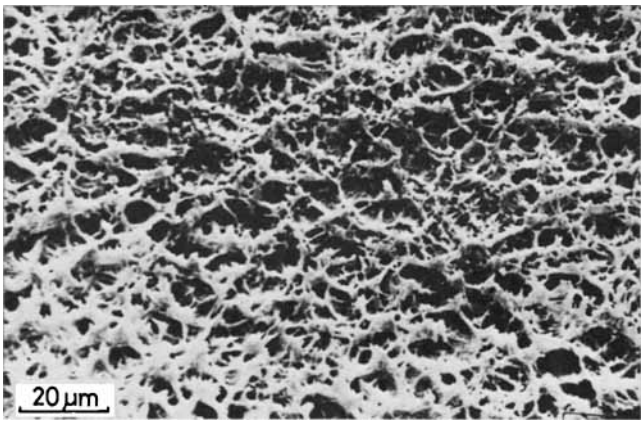

Fig. 15. High magnification SEI from the region near to the notch in which no fatigue cracks are visible: aged specimen.

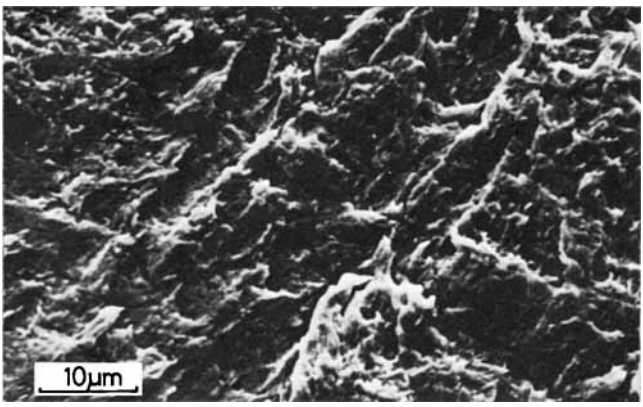

Fig. 16. High magnification SEI of another part of the fracture surface of the specimen shown in Figure 15, showing the appearance at a more advanced stage of cracking.

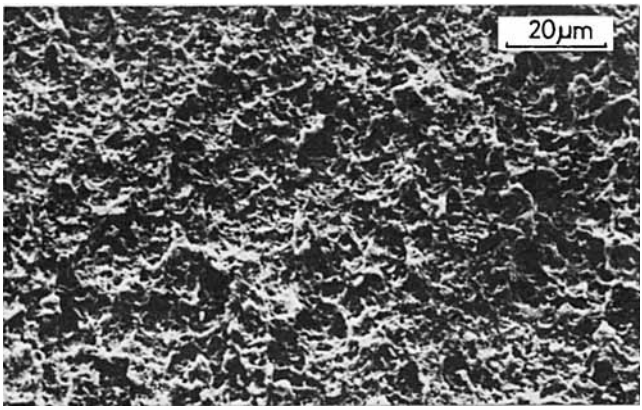

Fig. 17. Fracture surface from a uniaxial tensile failure using an unnotched aged specimen.

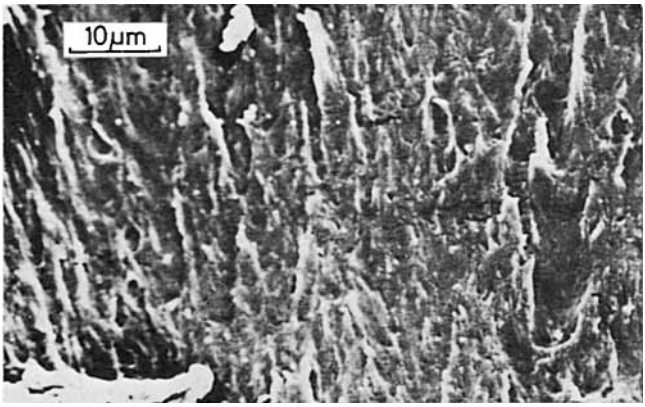

Fig. 18. High magnification SEI of a region remote from the notch of a notched specimen broken in uniaxial tension in a single pull.

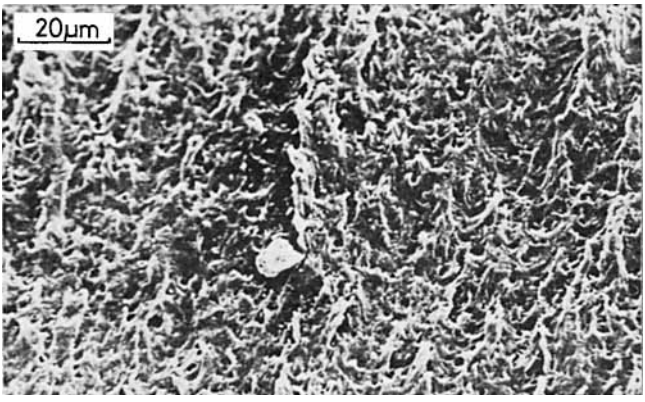

Fig. 19. Voided area near to the notch on the same fracture surface from which Figure 18 was taken.

DISCUSSION

The first point to be made is that the experiments described here have not revealed any major differences in fracture behavior between P4MP1 injection moldings in different states. It is necessary to examine the results in detail in order to detect any effect at all.

Consider first the effect of the residual stresses. The crack front stretches across the thickness of the specimen so that near to the surface of the bar the crack tip is in a region of compressive residual stresses with aged or mechanically preconditioned bars and this gives diminished net tensile stresses at all points. In the interior the residual stress is tensile, and the net stress is therefore higher than the applied stress. It is in this region that the crack is expected to grow more quickly anyway, because it will be at least partly under plane strain conditions. Visual observation during testing confirmed that the crack did indeed advance more rapidly in the center of the specimen, and the location of the crack front at various stages of growth can be clearly seen on fracture surfaces showing fatigue striations (Fig. 13). Thus, it is pertinent to consider the effect of the residual stresses in this region. One approach would be to attempt a point-by-point correction to all of the data points in Figures 9 and 11, taking into account the residual stress, as read from the corresponding distributions (Figs. 2 and 5). This would be extremely tedious and, in the presence of the scatter, hardly worthwhile. To assess the typical magnitude of the correction, let us take the example of a test run at 10 MN/m^2 maximum stress. The net stress in the interior will be equal to this plus the residual stress level at each particular location and will, of course, be a function of position; but taking the value to be say 12 MN/m^2 for aged samples and 12.5 MN/m^2 for mechanically preconditioned samples a rough estimate of the effect can be made. It is observed that (kcW_0) will be approximately proportional to stress (through its dependence on W_0), at least over fairly small ranges of stress, so that the shift in $\log(kcW_0)$ produced by correcting for residual tensile stresses of 2 MN/m^2 (aged) and 2.5 MN/m^2 (mechanically preconditioned) will be log 1.2 and log 1.25, respectively, i.e., 0.08 and 0.10. With reference to Figure 12 this relative shift of 0.02 brings the two corresponding lines into near coincidence. This procedure presupposes that it is the peak stress rather than the stress range that governs the crack growth rate.

On adopting the same procedure for the results obtained with annealed samples, it should first be noted that the stresses in the interior were found to be compressive, so that if an average of 0.5 MN/m^2 is taken to represent the residual compressive stresses in the interior, this must be subtracted from the applied stress, and it is again convenient to calculate the effect when the peak for an applied stress is 10 MN/m^2. This leads to a shift in $\log(kcW_0)$ of log 0.95, or -0.02. This shift, in combination with those estimated above for aged and mechanically preconditioned samples, again brings the lines in Figure 12 nearer to coincidence. In view of the large scatter and the approximate nature of this correction procedure, this cannot be taken as conclusive evidence that residual stresses alone cause differences in the fatigue fracture behavior of P4MP1 in the different states

investigated. It does indicate that residual stresses are a possible cause, and that it is unlikely that the effect of any other agencies can be easily detected from data obtained by experiments such as the ones conducted here.

A further point to consider is the effect of residual stresses on the shape of the fracture front. The crack tends to grow faster in the plane strain region in the center of the bar, and, if residual tensile stresses are present there, this effect should be enhanced; conversely, compressive stresses near the surface, in the plane stress region, can be expected to retard the crack growth rate. This argument leads to the prediction that for specimens containing the conventional residual stress distribution (compressive near the surface, tensile in the interior) the fracture front should be more tightly curved than would be the case in the absence of residual stresses. The effect of reversing the residual stress sense should be to retard the rate of crack growth in the interior of the bar and accelerate it near to the surfaces. Comparison of Figures 13 and 20 shows that this can indeed be observed for the striations on the fracture surface for the aged sample (Fig. 13) are much more tightly curved almost up to the surface whereas the annealed sample which has tensile stresses at the surface and compressive stresses in the interior shows reduced and, at some points, reversed curvature regions near to the surface (Fig. 20).

Although the major purpose of this work was to study the effect of various thermomechanical histories on the fatigue fracture behavior of P4MP1, the investigation has necessarily involved an examination of the relaxation and aging behavior. The response of the material to stress has been found to be quite conventional, and in both compression-molded form and injection-molded form sigmoidal plots of (applied) stress vs. log time were obtained in stress–relaxation tests. The material was thus found to behave similarly to many other thermoplastics, (an exception is polyethersulfone[33]), and it is thus to be expected that the residual stresses will diminish on room temperature aging, as observed. It was expected similarly that annealing would reduce the residual stress levels still further, as found with other

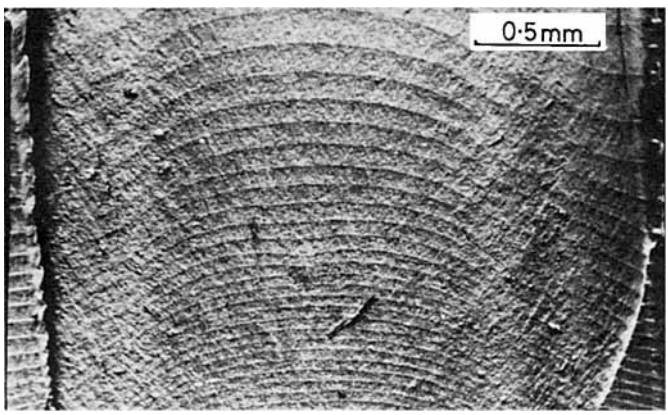

Fig. 20. Fatigue striations on the fracture surface of an annealed specimen, showing reduced and reversed curvature.

materials, but the reversal of the sense of stress was not anticipated. This is not an entirely unique result, for tensile stresses have been observed at the surface of injection moldings after thermoshock treatment,[34] after conditioning in a temperature gradient,[35] and after weathering outdoors in a hot climate.[36] In each of the other cases a temperature gradient was present (or expected to be present) across the molding during the post-molding treatment that promoted the change in stress. This fact is important in the explanation offered for the changes in stress observed to be caused by a controlled temperature gradient.[35] Essentially, it is proposed that stresses relax at least partially in the warmer side of a bar located between two plates held at different temperatures and that, when the bar subsequently cools down to room temperature thermal, shrinkage will be greatest near to the warm surface so that this part becomes tensile. More details are to be found in the paper by Thompson and White.[35] This hypothesis cannot be offered as an explanation for the development of tensile stresses at the surface of samples annealed at a uniform temperature, as under examination here. To account for the observed stress distribution, we can offer two possible explanations. Firstly, if the skin and core material have different coefficients of linear expansion, then on cooling down from the annealing temperature (at which it is expected that the stresses are reduced to a fairly low value), stresses will develop that result from differential thermal contraction. Secondly, if at the annealing temperature molecular orientation can be relaxed, some of the stress associated with this may be retained on subsequently cooling down; this mechanism may have a certain intuitive appeal, but is not a straightforward process and a quantitative assessment would require a knowledge of entropy elasticity, molecular mobility, and their interactions at all temperatures from room temperature to the annealing temperature and is beyond the scope of this paper.

The results obtained in this study do not provide any information on the aging characteristics of P4MP1 other than those connected with the relaxation of molding stresses. The characteristics and properties of most polymers change with post molding time. One of the most commonly monitored properties is volume, and densification is often observed on aging. P4MP1 presents a special case for it has an extremely low density ($\sim$835 kg/m^3 at room temperature) and furthermore because the density of the crystalline and noncrystalline phases are almost identical. At some temperatures (< 50°C) the crystal phase is less dense than the noncrystalline phase,[37,38] a property shared by no other polymer to our knowledge. These properties are the consequence of the rather loose helical arrangement of molecules within the crystals. Given the similar densities of the ordered (crystalline) and disorganized phases, it would seem that there may be little scope for changes in the density of the noncrystalline material by modest rearrangements within the noncrystalline phase of the kind associated with physical aging of amorphous polymers and not much change in the thermodynamic state variables. Perhaps, then, it should be anticipated that during aging the amount of structural reorganization occurring, and hence the extent of property change, should be rather modest with this material. With hindsight it therefore appears that this material could be a good choice for studying the effect of residual stress, for this may be easier to isolate than

with materials which age markedly as a result of any treatment applied to modify the residual stresses. Such a conclusion can only be regarded as tentative in the absence of more information.

The residual stress profile in cyclically loaded specimens showed an increase in stress magnitudes. The cyclic loading inhibited relaxation of the residual stresses, consistent with the idea that aging-related changes are retarded. The observed increase is not easy to explain. It has been demonstrated above that fatigue fracture crack growth rate variations between specimens in different states may simply relate to the different residual stress levels.

CONCLUSIONS

The fatigue fracture behavior of injection-molded P4MP1 is not very sensitive to post-molding conditioning. Small but significant differences were observed and can be explained by differences in residual stresses that develop during post-molding treatments. The fracture surfaces showed drawing similar to that found with other semicrystalline polymers when tested under similar conditions. Aging at room temperature makes very little difference to the residual stresses or stress–relaxation behavior of P4MP1, but cyclic loading caused an increase in residual stress level. Elevated temperature conditioning caused a reversal in the sense of the residual stresses, and an explanation has been offered in terms of differential thermal contraction of the skin and core. Depressed temperature aging (−18°C) also promoted a significant change in the residual stress distribution, but we cannot offer an explanation for this at the present time.

G. J. S. wishes to acknowledge the support provided by a SERC studentship. Further support for the purchase of equipment and consumables was also provided by SERC.

References

1. J. R. White, *Polym. Testing*, **4**, 165, (1984).
2. L. C. E. Struik, *Physical Aging in Amorphous Polymers and Other Materials*, Elsevier, Amsterdam, 1978.
3. D. R. Moore and S. Turner, *Phys. Technol.*, **5**, 177 (1974).
4. E. H. Andrews and B. J. Walker, *Proc. Roy. Soc., London*,**A325**, 57 (1971).
5. D. M. Gezovich and P. H. Geil, *Polym. Eng. Sci.*, **8**, 202 (1968).
6. C. K. Chai and N. G. McCrum, *Polymer*, **21**, 706 (1980).
7. C. K. Chai and N. G. McCrum, *Polymer*, **25**, 291 (1984).
8. L. D. Coxon and J. R. White, *Polym. Eng. Sci.*, **20**, 230 (1980).
9. J. W. Teh, J. R. White, and E. H. Andrews, *J. Mater. Sci.*, **10**, 1626 (1975).
10. J. W. Teh, J. R. White, and E. H. Andrews, *Polymer*, **20**, 755 (1979).
11. J. R. White and J. W. Teh, *Polymer*, **20**, 764 (1979).
12. J. F. Mandell, K. L. Smith, and D. D. Huang, *Polym. Eng. Sci.*, **21**, 1173 (1981).
13. M. H. Sadd, S. G. McDaniel, and K. E. Tucker, *Int. J. Fract.*, **14**, R253 (1978).
14. J. Bowman, N. Harris, and M. Bevis, *J. Mater. Sci.*, **10**, 63 (1975).
15. J. Bowman and M. Bevis, *Plast. Rubb. Maters. Appl.*, **1**, 177 (1976).
16. B. Haworth, C. S. Hindle, G. J. Sandilands, and J. R. White, *Plast. Rubb. Proc. Appl.*, **2**, 59 (1982).
17. R. G. Treuting and W. T. Read Jr, *J. Appl. Phys.*, **22**, 130 (1951).
18. G. J. Sandilands, PhD thesis, University of Newcastle upon Tyne, 1983.
19. B. Haworth, MSc thesis, University of Newcastle upon Tyne, 1980.
20. J. R. White, *J. Mater, Sci.*, **20**, 2377 (1985).

21. W. Knappe, *Kunststoffe,* **51**, 562 (1961); *Kunststoffe: German Plast.* **51**, 56 (1961).
22. A. I. Isayev, C. A. Hieber, and D. L. Crouthamel, SPE 39th Antec, Boston, 1981, p. 110.
23. A. I. Isayev and C. A. Hieber, *Rheol. Acta,* **19**, 168 (1980).
24. J. G. Williams, *Plast. Rubb. Proc. Appl.* **1**, 369 (1981).
25. N. J. Mills, *J. Mater. Sci.,* **17**, 558 (1982).
26. E. H. Andrews, "Testing of Polymers" **4**, 237 (1969) (Ed. W. E. Brown). Wiley Interscience, New York.
27. R. S. Rivlin and A. G. Thomas, *J. Polym. Sci.,* **10**, 291 (1953).
29. J. S. Harris and I. M. Ward, *J. Mater. Sci.,* **8**, 1655 (1973).
30. Y. W. Mai, *J. Mater. Sci.,* **9** 1896 (1974).
31. Y. W. Mai and J. G. Williams, *J. Mater. Sci.,* **14**, 1933 (1979).
32. R. W. Hertzberg, J. A. Manson, and M. Skibo, *Polym. Eng. Sci.,* **15**, 252 (1975).
33. M. M. Qayyum and J. R. White, J. Polym. Sci., *Polym. Lett. Ed.,* **21**, 31 (1983).
34. R. Krüger and H. Potente, *Polym. Eng. Rev.,* **1**, 19 (1981).
35. M. Thompson and J. R. White, *Polym. Eng. Sci.,* **24**, 227 (1984).
36. M. M. Qayyum and J. R. White, *J. Mater. Sci.,* **20**, 2557 (1985).
37. J. H. Griffith and B. G. Rånby, *J. Polym. Sci.,* **44**, 369 (1960).
38. M. Litt, *J. Polym. Sci.,* **A1**, 2219 (1963).

Received November 20, 1984
Accepted March 4, 1985